

# Nucleon-nucleon resonances at intermediate energies using a complex energy formalism.

G. Papadimitriou<sup>1,\*</sup> and J. P. Vary<sup>1,†</sup>

<sup>1</sup>*Department of Physics and Astronomy, Iowa State University, Ames, Iowa 50011-3160, USA*

We apply our method of complex scaling, valid for a general class of potentials, in a search for nucleon-nucleon S-matrix poles up to 2 GeV laboratory kinetic energy. We find that the realistic potentials JISP16, constructed from inverse scattering, and chiral field theory potentials N<sup>3</sup>LO and N<sup>2</sup>LO<sub>opt</sub> support resonances in energy regions well above their fit regions. In some cases these resonances have widths that are narrow when compared with the real part of the S-matrix pole.

PACS numbers: 21.45.Bc, 21.60.De, 24.10.-i

*Introduction.* There is a long-standing interest and considerable recent progress in the theoretical characterization of nuclear resonant states. A resonant state is fully characterized by its position in the energy plane and its width, which determines how fast the state will decay. One could in general solve the time-dependent Schrödinger equation to study the characteristics of resonant states [1–3], which is a demanding computational process. On the other hand, the time-independent many-body methods that deal with the description of resonant states in nuclei are under development and exhibit appealing computational features. These time-independent methods can be divided into real energy and complex energy approaches.

The spectrum of a real nuclear Hamiltonian consists of negative and positive energy states. While the negative energy spectrum is discrete (bound states), the positive energy spectrum may have a richer structure with resonant states among scattering or continuum states. Hence real-energy approaches require criteria for identifying a resonant structure and for assigning a position and a width to them.

In the domain of  $\mathcal{L}^2$  integrable basis expansion methods this is usually achieved through  $\mathcal{L}^2$  stabilization methods [4, 5] or methods that evaluate the real Continuum Level Density (CLD) [6]. The CLD usually produces an approximate Breit-Wigner distribution in the region of the resonant state whose parameters could be determined by a fit. The CLD method has been successfully applied to atomic systems [7], nuclear clusters [8] and in mean-field approaches for describing quasiparticle resonant states [9].

The name stabilization, arises from the fact that one does not need the knowledge of the asymptotic wavefunction in order to determine the resonant parameters. On the reaction side, based on R-matrix considerations [10–12], and assuming the single channel approximation, resonant parameters can be determined by the behavior of the phase-shift function of energy  $\delta(E)$  around the resonant position; in particular the position is defined as the inflection point of  $\delta(E)$  (maximum energy derivative of  $\delta(E)$ ) and the width is defined as  $\Gamma = \frac{2}{d\delta/dE}|_{E=E_r}$ , where

$E_r$  is the inflection point. Such formulas were employed recently in microscopic R-matrix calculations [13] to extract widths from realistic nucleon-nucleus phase-shifts. Though the R-matrix parametrizations have been very successful, the formulas become less transparent in the multi-channel case and when they are applied for the description of broad resonances (see discussion in [14]). Furthermore, for broad resonances, R-matrix analyses become more dependent on channel radii and boundary conditions [15]. Finally, combining formulas and assumptions from different theories/models for the calculation of an observable increases the possibility of uncontrollable errors.

The complex energy formalism serves as a potentially fruitful alternative for the characterization of the resonant parameters. It has been shown that once the R-matrix, S-matrix and T-matrix are analytically continued to the complex energy plane, the extraction of resonant parameters becomes independent of boundaries and radii [16]. Apart from this practical issue, some physical phenomena may have a more natural interpretation once the theory is developed in the complex energy plane (e.g. thermo-nuclear reactions [17, 18]). In the complex energy formalism, the Gamow (resonant) states, i.e. the solutions of the Schrödinger equation which satisfy purely outgoing boundary conditions (complex wave number  $k$ ), play a dominant role. It was shown by Berggren [19] that resonant states, when accompanied by non-resonant continuum states, form a complete set, an important property that gives rise to Berggren basis expansion methods either in a Configuration Interaction (CI) framework [20–25], Coupled Cluster framework [26–28] or reaction theory framework [29–35]. Expressing the Hamiltonian in such a complex energy, orthonormal non  $\mathcal{L}^2$  integrable basis, automatically allows its spectrum to support resonant and also non-resonant continuum states. In addition, when the Berggren basis is used in a reaction framework the detailed knowledge of the boundary condition at large distances is not crucial.

The Complex Scaling (CS) method also belongs in the category of complex energy formalisms. The Aguilar-Balslev-Combes (ABC) theorem [36, 37] establishes that

once the Hamiltonian coordinates are rotated, the resonant states are independent of the rotation and behave asymptotically as bound states. Consequently, one could use the technology that has been established for bound states in order to describe resonant and scattering phenomena. Furthermore, the CS method has been successfully applied in nuclear physics [38–42] (see also [43] for an application of CS in a deformed nuclear mean-field). We recently showed [44] that this method may be applied to the most general cases of non-local nuclear potentials.

In this work we apply the CS method to nucleon-nucleon (NN) scattering spanning the range from threshold to 2 GeV laboratory kinetic energy, which exceeds the fitting range of most NN potentials. We elect to retain non-relativistic kinematics throughout as the interactions are derived for a non-relativistic scattering framework. We employ three different realistic NN interactions and we find resonant poles at laboratory kinetic energy of about 600 MeV, or at about 2.2 GeV in the total center of mass energy. Some of these poles correspond to narrow resonant states.

According to the SAID data analysis group [45–47] (see also [48]) there exist resonance-like structures, poles of the S-matrix, in the  $^1D_2$ ,  $^3F_3$  uncoupled and coupled  $^3P_2$ - $^3F_2$  channels. Recently a resonant-like structure was also found by the WASA-at-COSY collaboration and the SAID analysis group in the  $^3D_3$ - $^3G_3$  coupled channel [49, 50]. Our CS calculations, in addition to showing resonances in these channels, also reveal resonance-like structures in the  $^3P_0$  and  $^3P_1$  channels. We searched other channels up to and including  $L=4$  without any additional signals of resonance-like structures.

The study of dibaryon resonances could shed light on the reaction mechanism and aid in the interpretation of excited nucleonic states. It is also valuable to pin down the properties of dibaryon resonances as a potential link between Quantum Chromodynamics, hadron models and traditional low energy nuclear physics. In the work of [45–47] the resonant-like structures were identified by analytically continuing the T-matrix of the available data in the complex energy plane. Our goal is to simply identify resonant structures with the CS method but not to study in depth the characteristics of the NN scattering at intermediate energies, something that would require the use of NN interactions that fit scattering data at higher energies, such as CDBonn [51] or AV18 [52]. Such in-depth studies would be done relativistically [53] and by treating properly  $\Delta$  and/or Roper resonances degrees of freedom (see for example [54]). Furthermore, we will not provide information on the possible decay paths that the resonant structures will follow, since we do not consider couplings to inelastic channels such as,  $NN \rightarrow \pi d$  or  $NN \rightarrow \Delta N$  etc. In addition, the interactions we use, are modeling the short-range (high-energies) NN sector in different approaches and are fitted at lower laboratory energies ( $\leq 350$  MeV). Hence, we are not aiming

at making predictions for the existence or absence of broad dibaryonic states. Nevertheless, it is worthwhile to discover that the NN interactions we employ, support high energy resonant-like states above the  $\Delta$  production threshold (1232 MeV). The existence of these resonances indicates such degrees of freedom suggest it may be important to examine what effect the explicit inclusion of the related degrees of freedom will have on finite nuclei. Simply stated, our goal at this point is to demonstrate that the CS method locates these resonances using three different realistic NN interactions in the conventional non-relativistic framework.

*Method and results.* We apply the CS transformation to our Hamiltonian which consists of the relative kinetic energy  $T$  and the realistic NN interaction  $V$  between the nucleons. The complex rotated Hamiltonian has the form:

$$H(r, \theta) = e^{-2i\theta}T + V(re^{i\theta}), \quad (1)$$

where  $\theta$  is the real CS rotation parameter. Nuclear potentials are usually non-local in coordinate space but, for simplicity and compactness, the potential is taken to be local in Eq.(1). In [44] we presented our methodology (see also [55]) for applying the CS transformation to a non-local potential which we also follow here. The time-

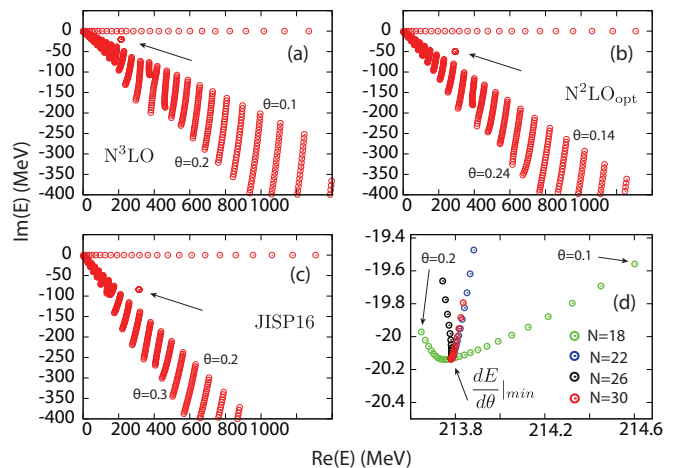


FIG. 1. (Color online) Spectrum of the CS Hamiltonian (1) for the  $N^3LO$  (a),  $N^2LO_{opt}$  (b) and JISP16 realistic potentials for the  $^3P_1$  channel (or  $1^-$  state) of the  $np$  system. There is a state that is invariant of the rotation angle  $\theta$  (rad), indicated by an arrow. In panel (d) we show a magnification of the  $N^3LO$  Hamiltonian spectrum in the region of the resonant-like state at a sequence of cutoffs in the number of radial nodes ( $N$ ) in the basis. This is the  $\theta$ -trajectory. Energies are in the Center of Mass (CoM) frame.

independent non-relativistic Schrödinger equation then becomes:

$$H(r, \theta)\Psi(r, \theta) = E(\theta)\Psi(r, \theta). \quad (2)$$

where  $E$  is the energy in the Center of Mass (CoM) frame here and throughout this work. To be more precise,

the rotated non-Hermitian Hamiltonian operator and the Hermitian one, are related through the formula:

$$H(r, \theta) = U(\theta)H(r)U(\theta)^{-1}, \quad (3)$$

where  $U(\theta)$  stands for the non-Unitary CS transformation operator. It is then expected that any quantum mechanical operator  $O$  will be transformed under (3) in the case of CS (e.g. see [56] for an application on the dipole operator). In order to calculate its expectation value, one could either use the transformed operator and calculate its expectation value between CS solutions ( $\theta \neq 0.0$ ), or evaluate the bare operator and calculate its expectation value using the coefficients from the back-rotated,  $\theta$ -independent solution. In [42] it was shown that both ways are equivalent and, in addition, the back-rotation transformation was stabilized via a smoothing process.

In order to solve Eq.(2) we assume that the solution is a linear combination of orthonormal Harmonic Oscillator (HO) basis states and we solve a complex symmetric Hamiltonian eigenvalue problem by diagonalization. The spectrum of the Hamiltonian contains resonant (bound states, resonances) and non-resonant continuum states. According to the ABC theorem, once the resonant state is revealed it remains invariant under CS rotations, whereas the non-resonant continuum states follow an approximate  $2\theta$  path in the complex energy plane. This is the complex stabilization criterion that is used in CS for the identification of the resonant state. In practice, due to the truncation of the underlying basis, there is a small variation of the resonant position with  $\theta$ . It is then a consequence of the complex virial theorem [57] that the resonant state will be the one that corresponds to the minimal change of the real part of the energy with respect to  $\theta$ . The method is also known as  $\theta$ -trajectory method and it is a common practice in CS applications (see for example [42, 58, 59]). We also apply this stabilization technique and we check convergence of our results as a function of the basis dimension and the variations with the rotation angle.

In Fig.1 we present the spectrum of the complex scaled Hamiltonian for the  $^3P_1$  ( $1^-$ ) channel of the neutron-proton ( $np$ ) system, for the JISP16 [60] and the two chiral effective field theory interactions  $N^3LO$  [61] and  $N^2LO_{opt}$  [62]. The HO basis was characterized by  $\hbar\omega = 40$  MeV for JISP16 and  $N^2LO_{opt}$  and by  $\hbar\omega = 28$  MeV for  $N^3LO$ . For the  $N^3LO$  potential we varied the rotation from  $\theta = 0.1$  rad to  $0.2$  rad, for  $N^2LO_{opt}$  from  $\theta = 0.14$  to  $0.24$  rad and for JISP16 from  $\theta = 0.2$  to  $0.3$  rad. The step in the  $\theta$  discretization was  $0.004$  rad. As we start rotating the coordinates and momenta of the Hamiltonian, solutions that initially inhabit the real-axis ( $\theta = 0.0$ ) start moving inside the complex energy plane. During the rotation, when a state crosses the ordinates of a pole of the S-matrix, it remains there and does not follow the rotation of the other non-resonant continuum states. In Fig.1 we see clearly that all interactions support one

state which is almost invariant with respect to the CS rotation parameter. For the calculations in panels (a), (b) and (c) we used a HO basis that consisted of a maximum of  $N=30$  radial nodes. The resonant parameters of this state were identified by applying the  $\theta$ -trajectory method. Any Hamiltonian after the CS transformation is applied, becomes non-Hermitian and one needs to locate the resonant state or the stationary point. The stationary point is the one for which the difference in energy with respect to the  $\theta$  variation is minimal. The  $\theta$ -trajectory is shown in panel (d) of Fig.1. We see that for each basis

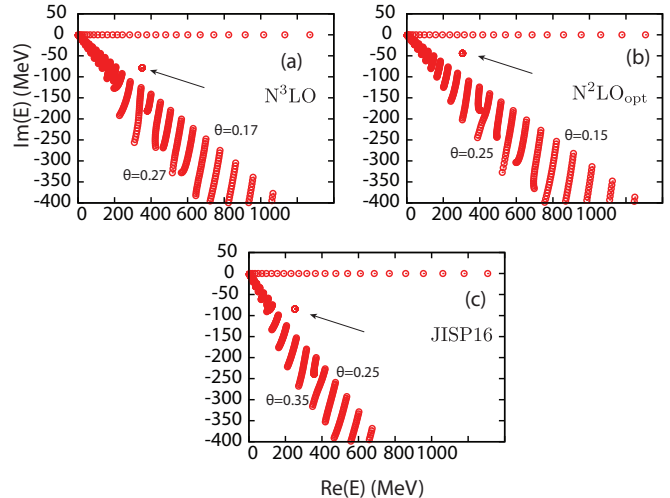


FIG. 2. (Color online) Same as Fig.1 but for the  $^3P_0$  channel ( $0^-$  state) and for a HO basis size of  $N=30$ .

size (denoted by  $N$ ) the  $\theta$ -trajectory is different. Nevertheless, the variations become smaller by increasing the basis size and the results for  $N=26$  and  $N=30$  start to coincide for  $\theta > 0.17$  rad. At this point we also notice that results are practically converged at  $N=18$  and differences appear only in the fifth and sixth significant digit.

In addition to the  $\theta$ -trajectory method, the b-trajectory method is employed [58] in CS calculations. This b-trajectory method uses the dependence of the results on the length parameter of the basis, in our case the HO length or, equivalently,  $\hbar\omega$ . We do not analyze the b-trajectory method here. Here, we simply note that the deuteron ground state (g.s.) ( $^3S_1$ - $^3D_1$  coupled channel) is very well converged (independent of  $\hbar\omega$ ) at  $N = 30$ . We will perform detailed b-trajectory analyses in future applications of CS to resonances in finite nuclei.

We gather a sample of our results for the  $^3P_1$  state in Table I. The sensitivity analysis regarding the  $\theta$  dependence and the basis convergence was also performed for the other partial waves.

In Fig.2 we present the CS spectrum for the  $^3P_0$  channel. For a basis size of  $N=30$  the converged resonant-like states are  $(350.859 - i78.689)$  MeV,  $(305.859 - i44.827)$  MeV and  $(251.252 - i84.454)$  MeV for the  $N^3LO$ ,  $N^2LO_{opt}$

TABLE I.  $^3P_1$  resonant parameters in MeV as a function of the HO basis size. The choice of the energy was decided by the  $\theta$ -trajectory method. The energies are in the CoM of the  $np$  system above the  $np$  threshold ( $E=0$ ). To obtain the width, the formula  $\Gamma = -2\text{Im}(E)$  could be applied. For the  $np$  system the nucleon mass is taken to be  $938.2 \text{ MeV}/c^2$ .

N	N <sup>3</sup> LO	N <sup>2</sup> LO <sub>opt</sub>	JISP16
14	(214.767 -i20.048)	(292.114 -i49.609)	(314.471 -i84.250)
18	(213.758 -i20.139)	(292.358 -i50.039)	(314.475 -i84.244)
22	(213.784 -i20.131)	(292.323 -i50.023)	(314.473 -i84.244)
26	(213.781 -i20.134)	(292.327 -i50.020)	(314.473 -i84.244)
30	(213.781 -i20.134)	(292.327 -i50.020)	(314.473 -i84.244)

and JISP16 interactions respectively.

We now focus our attention on the N<sup>3</sup>LO and JISP16 interactions, since they are both fitted to higher ener-

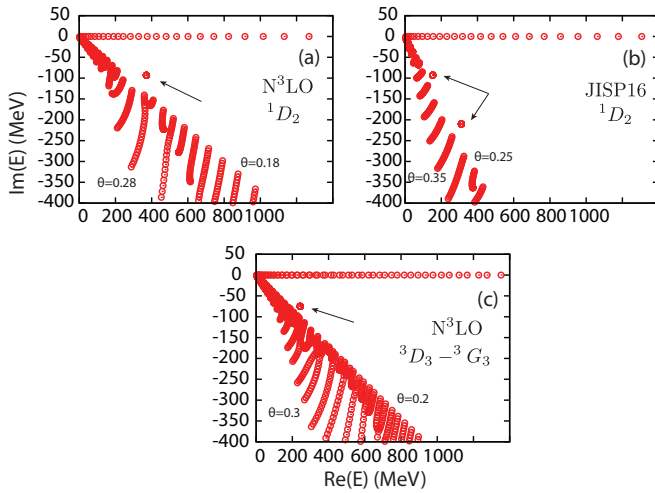


FIG. 3. (Color online) Spectrum of the  $^1D_2$  channel with the N<sup>3</sup>LO (a) and JISP16 (b) interactions. Notice the two poles in the case of JISP16. In panel (c) it is the coupled  $^3D_3$ - $^3G_3$  spectrum for the N<sup>3</sup>LO interaction.

gies than N<sup>2</sup>LO<sub>opt</sub>. The  $^1D_2$  channel shown in Fig. 3 presents an interesting case since both interactions support resonant states and, in the case of JISP16, we find two resonances. According to our calculations the N<sup>3</sup>LO resonant position is at (371.111 -i93.169) MeV. We notice that at an energy of about 400 MeV for the real part and about -150 MeV for the imaginary part, there is also a state that shows a stabilization pattern with respect to the rotation parameter. This state, however, is not as stable as the other cases we examine in this work, so we do not investigate it further. For the JISP16 interaction we observe clearly two resonant positions in the  $^1D_2$  channel : (153.155 -i92.725) MeV and a broader structure at (311.008 -i210.065) MeV (see panels (a) and (b) of Fig. 3).

In panel (c) of Fig.3 we show the spectrum for the cou-

pled  $^3D_3$ - $^3G_3$  channel for the N<sup>3</sup>LO potential which supports a resonant state at a position: (219.218 -i75.162) MeV. For the same channel, not shown here, the JISP16 interaction supports a broader structure at (200.084 -i115.138) MeV. In this JISP16 case the rotation angle was varied from  $\theta = 0.32$  to  $0.42$  rad in order to reveal the broader resonant position.

In Fig. 4 we show our results for the uncoupled  $^3F_3$  and the coupled  $^3P_2$ - $^3F_2$  channels using the N<sup>3</sup>LO and JISP16 forces. For these partial waves we find multiple resonances supported by the interactions. The chiral potential supports at least four resonant-like structures for the  $^3F_3$  channel and for the coupled  $^3P_2$ - $^3F_2$  channel, where in the latter case we also see some indications for resonant structures at energies larger than 400 MeV CoM. According to our calculations, for the JISP16 interaction we find two resonant-like structures for each of the  $^3F_3$  and  $^3P_2$ - $^3F_2$  channels. After applying the  $\theta$ -

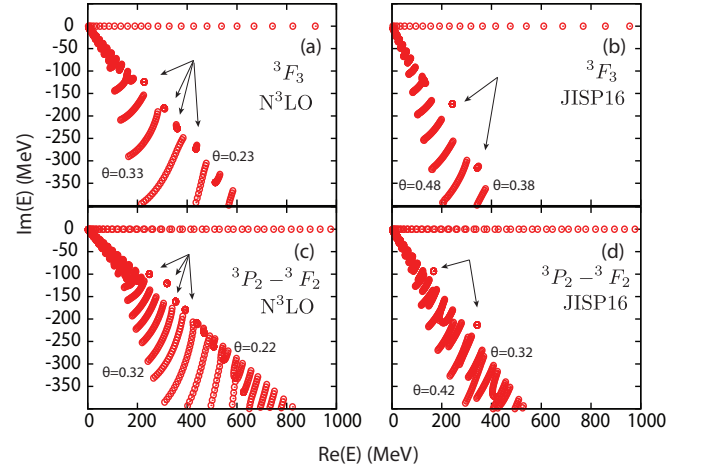


FIG. 4. (Color online) Same as in Fig. 3 but for the  $^3F_3$  channel (panels (a),(b)) and  $^3P_2$ - $^3F_2$  (panels (c),(d)) for the N<sup>3</sup>LO and JISP16 interactions respectively. See also Table II.

TABLE II. Resonant parameters that correspond to the arrows of Fig. 4, computed with the  $\theta$ -trajectory method for the uncoupled  $^3F_3$  and coupled  $^3P_2$ - $^3F_2$  channels, using the N<sup>3</sup>LO and JISP16 interactions.

N <sup>3</sup> LO		JISP16	
$^3F_3$	$^3P_2$ - $^3F_2$	$^3F_3$	$^3P_2$ - $^3F_2$
(227.0 -i124.3)	(247.8 -i99.8)	(242.3 -i173.4)	(161.2 -i95.2)
(307.2 -i182.5)	(318.9 -i120.5)	(342.6 -i315.6)	(342.4 -i213.2)
(360.5 -i227.9)	(353.5 -i160.6)		
(435.3 -i273.2)	(392.0 -i179.1)		

trajectory stabilization method we gather the results in Table II. We notice that the states are broader than the structures we find for the  $^3P_0$  and  $^3P_1$  channels. The positions of the resonant states in each channel depend on the interaction we use. In this sense, the situation is



distinctly different from the deuteron ground state that all the realistic NN interactions are constrained to describe with high accuracy. Of course, this dependence of the scattering resonances on the NN interaction may be expected since we are investigating a kinematic region which is sensitive to short range nuclear physics, a sector that each NN interaction models differently.

To show that the resonance locations are fixed by NN model assumptions and not by the couplings of low and high momenta alone, we made a test which demonstrates that the  $^3P_1$  resonant state for the  $N^3LO$  potential is invariant under similarity renormalization group (SRG) transformations [63], down to a scale of  $\lambda = 1.5\text{fm}^{-1}$ . A scale of  $\lambda = 1.5\text{fm}^{-1}$ , taken as a maximum relative momentum, corresponds roughly to an energy of 187 MeV in the laboratory frame. The real part of energy of the  $^3P_1$  resonant-like state (see Table I) is above the energy implied by this SRG scale (i.e.  $E_{res}^{lab} \sim 2 \cdot 214 = 428$  MeV). Intuitively, one would think that the NN physics up to this SRG scale will remain invariant but above this scale one might expect some changes so we are motivated to test for SRG scale invariance using this resonance as the test case.

Using the  $N^3LO$  interaction in the  $^3P_1$  channel we performed three SRG transformations, that reduce the couplings of low momentum to high momentum states and change the off-shell components of the potential, leaving the on-shell properties invariant. In Fig.5 we observe that the position of the  $^3P_1$  resonant-like state is invariant under these SRG evolutions, for the SRG transformation scale as low as  $\lambda = 1.5\text{fm}^{-1}$  starting from a bare  $N^3LO$  potential. For these calculations the rotation angle was rotated from  $\theta = 0.1$  rad to  $0.2$  rad with a step of  $0.05$  rad.

**Conclusions.** In this work we applied the CS method to study resonant features of the NN interaction in energy regions above the usual 300 to 350 MeV laboratory energy. While this region exceeds the energies for which these non-relativistic interactions are developed, we obtain resonances motivating further exploration and we demonstrate the robust characteristics of our techniques.

We analyzed the resonant features that we found in several channels and we studied the stability of the results using the  $\theta$ -trajectory method whose validity has been demonstrated for local and schematic potentials. In our work we find similar convergence patterns for resonant states to what other authors have found. Among the numerous NN resonances that we found, the one in the  $^3P_1$  channel appeared close to the real energy axis.

In our formalism, the widths of the states should be viewed as total decay widths, and since we did not consider special decay channels in our analysis, we cannot say if the  $np$  system will decay by either emitting mesons or baryon resonances. Our numerical results show that the positions of these states in the complex plane depend strongly on the form of the underlying interac-

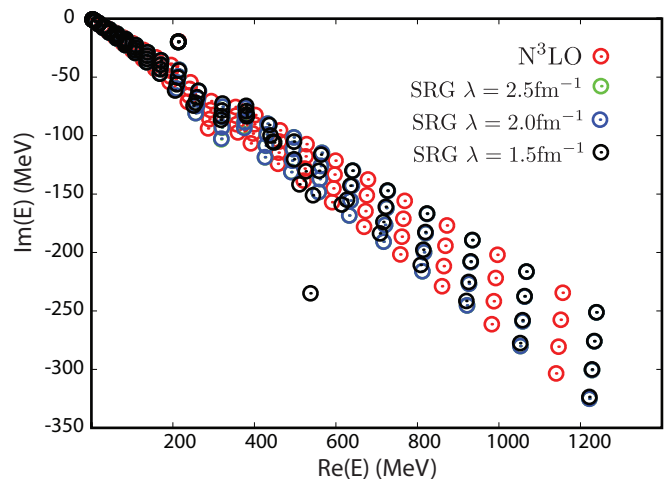


FIG. 5. (Color online)  $^3P_1$  channel CS spectrum for the bare  $N^3LO$  force and for three different SRG evolution scales. The resonant-like structure remains invariant. The green circle that corresponds to SRG  $\lambda = 2.5\text{fm}^{-1}$  practically overlaps with the results of the other SRG evolution scales and it is not visible. A solution is observed that corresponds to a  $\lambda = 1.5\text{fm}^{-1}$  with an imaginary part of about  $-250$  MeV. This is a non-resonant continuum state which happened to depart from the approximate  $2\theta$  line.

tion. Hence these NN-dependent S-matrix poles are distinguished from the deuteron pole whose properties are shared by all realistic NN interactions to high accuracy.

We focused on a specific force in one channel, in particular the chiral  $N^3LO$  in the  $^3P_1$  channel, to demonstrate that the position of the resonant-like state is invariant under the action of SRG transformations.

Finally, it worth mentioning that analysis of NN scattering data has not, to our knowledge, reported resonant poles for the  $^3P_0$  and  $^3P_1$  partial waves, but rather for the  $^1D_2$ ,  $^3F_3$ ,  $^3P_2$ - $^3F_2$  and recently for the  $^3D_3$ - $^3G_3$ .

Among our achievements, we have demonstrated the stability of the CS method for identifying resonant states. This demonstration helps support the adoption of these techniques for investigating resonances in finite nuclei where we anticipate the interest will be in low-energy applications.

**Acknowledgements.** We gratefully acknowledge valuable discussions with I. I. Strakovsky. This work was supported by the US DOE under grants No. DESC0008485 (SciDAC/NUCLEI) and DE-FG02-87ER40371.

\* georgios@iastate.edu

† jvary@iastate.edu

- [1] P. Talou, D. Strottman, and N. Carjan, Phys. Rev. C **60**, 054318 (1999).
- [2] T. Maruyama, T. Oishi, K. Hagino, and H. Sagawa, Phys. Rev. C **86**, 044301 (2012).

- [3] A. Volya, Phys. Rev. C **79**, 044308 (2009).
- [4] A. U. Hazi and H. S. Taylor, Phys. Rev. A **1**, 1109 (1970).
- [5] R. Salzgeber, U. Manthe, T. Weiss, and C. Schlier, Chemical Physics Letters **249**, 237 (1996).
- [6] S. Shlomo, Nuclear Physics A **539**, 17 (1992).
- [7] A. T. Kruppa and K. Arai, Phys. Rev. A **59**, 3556 (1999).
- [8] K. Arai and A. T. Kruppa, Phys. Rev. C **60**, 064315 (1999).
- [9] J. C. Pei, A. T. Kruppa, and W. Nazarewicz, Phys. Rev. C **84**, 024311 (2011).
- [10] A. Arima and S. Yoshida, Nuclear Physics A **219**, 475 (1974).
- [11] A. M. Lane and R. G. Thomas, Rev. Mod. Phys. **30**, 257 (1958).
- [12] P. Descouvemont and D. Baye, Reports on Progress in Physics **73**, 036301 (2010).
- [13] S. Baroni, P. Navrátil, and S. Quaglioni, Phys. Rev. C **87**, 034326 (2013).
- [14] I. J. Thompson and F. Nunes, *Nuclear Reactions for Astrophysics Principles, Calculation and Applications of Low-Energy Reactions, page 302* (Cambridge University Press, 2009).
- [15] A. Csótó and G. M. Hale, Phys. Rev. C **55**, 536 (1997).
- [16] D. Tilley, C. Cheves, J. Godwin, G. Hale, H. Hofmann, J. Kelley, C. Sheu, and H. Weller, Nuclear Physics A **708**, 3 (2002).
- [17] G. M. Hale, R. E. Brown, and N. Jarmie, Phys. Rev. Lett. **59**, 763 (1987).
- [18] A. Csótó, R. G. Lovas, and A. T. Kruppa, Phys. Rev. Lett. **70**, 1389 (1993).
- [19] T. Berggren, Nucl. Phys. A **109**, 265 (1968).
- [20] N. Michel, W. Nazarewicz, M. Płoszajczak, and K. Benaceur, Phys. Rev. Lett. **89**, 042502 (2002).
- [21] R. Id Betan, R. J. Liotta, N. Sandulescu, and T. Vertse, Phys. Rev. Lett. **89**, 042501 (2002).
- [22] J. Rotureau, N. Michel, W. Nazarewicz, M. Płoszajczak, and J. Dukelsky, Phys. Rev. Lett. **97**, 110603 (2006).
- [23] N. Michel, W. Nazarewicz, M. Płoszajczak, and T. Vertse, J. Phys. G: Nucl. Part. Phys. **36**, 013101 (2009).
- [24] R. I. Betan and W. Nazarewicz, Phys. Rev. C **86**, 034338 (2012).
- [25] G. Papadimitriou, J. Rotureau, N. Michel, M. Płoszajczak, and B. R. Barrett, Phys. Rev. C **88**, 044318 (2013).
- [26] G. Hagen, D. Dean, M. Hjorth-Jensen, and T. Papenbrock, Physics Letters B **656**, 169 (2007).
- [27] G. Hagen, M. Hjorth-Jensen, G. R. Jansen, R. Machleidt, and T. Papenbrock, Phys. Rev. Lett. **108**, 242501 (2012).
- [28] G. Hagen, M. Hjorth-Jensen, G. R. Jansen, R. Machleidt, and T. Papenbrock, Phys. Rev. Lett. **109**, 032502 (2012).
- [29] A. T. Kruppa, B. Barmore, W. Nazarewicz, and T. Vertse, Phys. Rev. Lett. **84**, 4549 (2000).
- [30] A. T. Kruppa and W. Nazarewicz, Phys. Rev. C **69**, 054311 (2004).
- [31] Y. Jaganathen, N. Michel, and M. Płoszajczak, Journal of Physics: Conference Series **403**, 012022 (2012).
- [32] G. Hagen and N. Michel, Phys. Rev. C **86**, 021602 (2012).
- [33] R. I. Betan, Physics Letters B **730**, 18 (2014).
- [34] K. Fosse, N. Michel, W. Nazarewicz, M. Płoszajczak, and Y. Jaganathen, Phys. Rev. A **91**, 012503 (2015).
- [35] K. Fosse, N. Michel, M. Płoszajczak, Y. Jaganathen, and R. Betan, (2015), nucl-th/1502.01631v2.
- [36] J. Aguilar and J. M. Combes, Commun. Math. Phys. **22**, 266 (1971).
- [37] E. Balslev and J. M. Combes, Commun. Math. Phys. **22**, 280 (1971).
- [38] B. Gyarmati and A. T. Kruppa, Phys. Rev. C **34**, 95 (1986).
- [39] T. Myo, Y. Kikuchi, H. Masui, and K. Katō, Progress in Particle and Nuclear Physics **79**, 1 (2014).
- [40] R. Lazauskas and J. Carbonell, Phys. Rev. C **84**, 034002 (2011).
- [41] H. Witala and W. Glöckle, Phys. Rev. C **60**, 024002 (1999).
- [42] A. T. Kruppa, G. Papadimitriou, W. Nazarewicz, and N. Michel, Phys. Rev. C **89**, 014330 (2014).
- [43] Q. Liu, J.-Y. Guo, Z.-M. Niu, and S.-W. Chen, Phys. Rev. C **86**, 054312 (2012).
- [44] G. Papadimitriou and J. P. Vary, Phys. Rev. C **91**, 021001 (2015).
- [45] R. A. Arndt, L. D. Roper, R. A. Bryan, R. B. Clark, B. J. VerWest, and P. Signell, Phys. Rev. D **28**, 97 (1983).
- [46] R. A. Arndt, J. S. Hyslop, and L. D. Roper, Phys. Rev. D **35**, 128 (1987).
- [47] R. A. Arndt, L. D. Roper, R. L. Workman, and M. W. McNaughton, Phys. Rev. D **45**, 3995 (1992).
- [48] I. Strakovsky, Fiz.Elem.Chast.Atom.Yadra **22**, 615 (1991).
- [49] P. Adlarson, W. Augustyniak, W. Bardan, M. Bashkanov, F. S. Bergmann, M. Berłowski, H. Bhatt, M. Büscher, H. Calén, I. Ciepał, H. Clement, D. Coderre, E. Czerwiński, K. Demmich, E. Doroshkevich, R. Engels, A. Erven, W. Erven, W. Eyrich, P. Fedorets, K. Föhl, K. Fransson, F. Goldenbaum, P. Goslawski, Goslawski, A. Goswami, K. Grigoryev, C.-O. Gullström, F. Hauenstein, L. Heijenskjöld, V. Hejny, M. Hodana, B. Höistad, N. Hüskén, A. Jany, B. Jany, L. Jarczyk, T. Johansson, B. Kamys, G. Kemmerling, F. Khan, A. Khokkaz, D. Kirillov, S. Kistryn, H. Kleines, B. Klos, M. Krapp, W. Krzemień, P. Kulesa, A. Kupś, K. Lalwani, D. Lersch, B. Lorentz, A. Magiera, R. Maier, P. Marciniowski, B. Mariański, M. Mikirtychiants, H.-P. Morsch, P. Moskal, H. Ohm, I. Ozerianska, E. Perez del Rio, N. Piskunov, P. Podkopał, D. Prasuahn, A. Pricking, D. Pszczel, K. Pysz, A. Pysznia, C. Redmer, J. Ritman, A. Roy, Z. Rudy, S. Sawant, S. Schadmand, T. Sefzick, V. Serdyuk, V. Serdyuk, R. Siudak, T. Skorodko, M. Skurzok, J. Smyrski, V. Sopov, R. Stassen, J. Stepaniak, E. Stephan, G. Sterzenbach, H. Stockhorst, H. Ströher, A. Szczurek, A. Täschner, A. Trzciński, R. Varma, G. Wagner, M. Wolke, A. Wrońska, P. Wüstner, P. Wurm, A. Yamamoto, L. Yurev, J. Zabierowski, M. Zieliński, A. Zink, J. Złomańczuk, P. Żuprański, M. Żurek, R. Workman, W. Briscoe, and I. Strakovsky ((WASA-at-COSY Collaboration) and (SAID Data Analysis Center)), Phys. Rev. Lett. **112**, 202301 (2014).
- [50] P. Adlarson, W. Augustyniak, W. Bardan, M. Bashkanov, F. S. Bergmann, M. Berłowski, H. Bhatt, M. Büscher, H. Calén, I. Ciepał, H. Clement, D. Coderre, E. Czerwiński, K. Demmich, E. Doroshkevich, R. Engels, A. Erven, W. Erven, W. Eyrich, P. Fedorets, K. Föhl, K. Fransson, F. Goldenbaum, P. Goslawski, A. Goswami, K. Grigoryev, C.-O. Gullström, F. Hauenstein, L. Heijenskjöld, V. Hejny, M. Hodana, B. Höistad, N. Hüskén,

- A. Jany, B. R. Jany, L. Jarczyk, T. Johansson, B. Kamys, G. Kemmerling, F. A. Khan, A. Khoukaz, D. A. Kirillov, S. Kistryn, H. Kleines, B. Kłos, M. Krapp, W. Krzemień, P. Kulesa, A. Kupść, K. Lalwani, D. Lersch, B. Lorentz, A. Magiera, R. Maier, P. Marciniewski, B. Mariański, M. Mikirtychiants, H.-P. Morsch, P. Moskal, H. Ohm, I. Ozerianska, E. Perez del Rio, N. M. Piskunov, P. Podkopał, D. Prasuhn, A. Pricking, D. Pszczel, K. Pysz, A. Pysznia, C. F. Redmer, J. Ritman, A. Roy, Z. Rudy, S. Sawant, S. Schadmand, T. Sefzick, V. Serdyuk, V. Serdyuk, R. Siudak, T. Skorodko, M. Skurzok, J. Smyrski, V. Sopov, R. Stassen, J. Stepaniak, E. Stephan, G. Sterzenbach, H. Stockhorst, H. Ströher, A. Szczurek, A. Täschner, A. Trzciński, R. Varma, G. J. Wagner, M. Wolke, A. Wrońska, P. Wüstner, P. Wurm, A. Yamamoto, L. Yurev, J. Zabierowski, M. J. Zieliński, A. Zink, J. Złomańczuk, P. Żuprański, M. Żurek, R. L. Workman, W. J. Briscoe, and I. I. Strakovsky (WASA-at-COSY Collaboration and SAID Data Analysis Center), *Phys. Rev. C* **90**, 035204 (2014).
- [51] R. Machleidt, *Phys. Rev. C* **63**, 024001 (2001).
- [52] R. B. Wiringa, V. G. J. Stoks, and R. Schiavilla, *Phys. Rev. C* **51**, 38 (1995).
- [53] W. N. Polyzou and C. Elster, *Journal of Physics G: Nuclear and Particle Physics* **41**, 094006 (2014).
- [54] A. A. Filin, V. Baru, E. Epelbaum, H. Krebs, C. Hanhart, and F. Myhrer, *Phys. Rev. C* **88**, 064003 (2013).
- [55] G. Hagen, J. S. Vaagen, and M. Hjorth-Jensen, *Journal of Physics A: Mathematical and General* **37**, 8991 (2004).
- [56] W. Horiuchi, Y. Suzuki, and K. Arai, *Phys. Rev. C* **85**, 054002 (2012).
- [57] E. Brändas, P. Froelich, and M. Hehenberger, *International Journal of Quantum Chemistry* **14**, 419 (1978).
- [58] S. Aoyama, T. Myo, K. Katō, and K. Ikeda, *Progress of Theoretical Physics* **116**, 1 (2006).
- [59] H. Masui, K. Katō, N. Michel, and M. Płoszajczak, *Phys. Rev. C* **89**, 044317 (2014).
- [60] A. Shirokov, J. Vary, A. Mazur, and T. Weber, *Physics Letters B* **644**, 33 (2007).
- [61] D. R. Entem and R. Machleidt, *Phys. Rev. C* **68**, 041001 (2003).
- [62] A. Ekström, G. Baardsen, C. Forssén, G. Hagen, M. Hjorth-Jensen, G. R. Jansen, R. Machleidt, W. Nazarewicz, T. Papenbrock, J. Sarich, and S. M. Wild, *Phys. Rev. Lett.* **110**, 192502 (2013).
- [63] S. K. Bogner, R. J. Furnstahl, and R. J. Perry, *Phys. Rev. C* **75**, 061001 (2007).